

## **CHAPTER 4.0: RESULTS**

### **4.1 Chemical analysis of soil and sediment samples**

The values of pH and the salinity of samples recorded were the average of two readings taken from each sample (Table 4.1).

The pH value of samples ranged from acidic (pH 5.9) to alkaline (pH 8.3). Marine sediments, beach soil, and melt lake sediment were moderately alkaline (pH 8.0 to pH 8.3) while inland lake bank sediments were slightly alkaline with an average pH of 7.85. Terrestrial soils were ranging from slightly acidic to moderate alkaline (pH 6.2 to pH 8.0) while periglacier soils were ranged from acidic to neutral (pH 5.9 to pH 7.3).

The salinity of samples was measured as electrical conductivity (EC). Salinity of marine sediments (1154.0  $\mu\text{S}/\text{cm}$  to 1705.0  $\mu\text{S}/\text{cm}$ ) were found to be higher than beach soil (304.0  $\mu\text{S}/\text{cm}$ ), terrestrial soils (72.7  $\mu\text{S}/\text{cm}$  to 506.0  $\mu\text{S}/\text{cm}$ ), inland lake bank sediments (130.4  $\mu\text{S}/\text{cm}$  to 273.3  $\mu\text{S}/\text{cm}$ ), melt lake sediment (70.4  $\mu\text{S}/\text{cm}$ ) and periglacier soils (1.1  $\mu\text{S}/\text{cm}$  to 32.3  $\mu\text{S}/\text{cm}$ ).

Table 4.1: The values of pH and salinity (EC) of soil and sediment samples

<b>Sample</b>	<b>Sample description</b>	<b>pH</b>	<b>EC<sup>a</sup> (μS/cm)</b>
1	Beach soil	8.0	304.0
3	Terrestrial soil	7.9	116.0
5	Terrestrial soil	7.5	156.1
8	Inland lake bank sediment	7.8	130.4
9	Terrestrial soil	6.2	506.0
17	Terrestrial soil	7.9	72.7
24	Marine sediment	8.1	1691.0
25	Marine sediment	8.1	1696.0
26	Marine sediment	8.1	1702.0
28	Marine sediment	8.3	1154.0
29	Marine sediment	8.2	1339.0
30	Marine sediment	8.3	1705.0
31	Periglacier soil	7.3	1.1
32	Periglacier soil	7.2	323.0
33	Periglacier soil	5.9	50.6
34	Terrestrial soil	6.4	95.6
35	Inland lake bank sediment	7.9	273.3
39	Melt lake sediment	8.2	70.4

<sup>a</sup> Electrical conductivity

## 4.2 Extraction of genomic DNA from soils and sediments

The genomic DNA from soils and sediments were successfully extracted using Ultra Clean™ Soil DNA Isolation Kit. The yield and purity of the extracted genomic DNA was measured by a biophotometer (Table 4.2).

The yield of genomic DNA that was extracted from the samples varied for all studied sites, ranging from 0.04 µg/µl to 3.584 µg/µl. The highest DNA yield (3.584 µg/µl) was measured for terrestrial soil collected from the rail track site (sample 3). Marine sediments from the 10 m depth site (samples 24, 25 and 26) have a lower DNA yield (0.040 µg/µl to 0.042) compared to marine sediments from the 20 m depth site (samples 28, 29 and 30) (0.089 µg/µl to 0.584 µg/µl).

The genomic DNA extracted from marine sediments with samples 24 ( $A_{260}:A_{280} = 1.98$ ) and 25 ( $A_{260}:A_{280} = 2.36$ ) have less protein contamination ( $A_{260}:A_{280} > 1.70$ ), compared to samples from other studied sites. The purity of extracted genomic DNA from all sites was poor, with humic acid contamination ( $A_{260}:A_{230} < 2.0$ ) ranging from  $A_{260}:A_{230} = 0.24$  to  $A_{260}:A_{230} = 1.14$ .

Comparison of DNA yield and purity of a sample with and without dilution of the extracted DNA are shown in Table 4.3. The amount of humic acid in undiluted extracted genomic DNA (sample 17) was high ( $A_{260}:A_{230} = 0.7$ ). However, with a 10-fold dilution of the extracted DNA, the amount of humic acid was reduced ( $A_{260}:A_{230} = 2.5$ ).

Table 4.2: Genomic DNA yield and purity from the samples (undiluted DNA extracts)

Sample	DNA yield ( $\mu\text{g}/\mu\text{l}$ )	$A_{260}:A_{280}$ <sup>a</sup>	$A_{260}:A_{230}$ <sup>b</sup>
1	0.979	1.12	0.88
3	3.584	1.01	0.93
5	0.052	1.49	0.57
8	0.239	1.38	1.13
9	0.073	1.30	0.61
17	0.052	1.11	0.70
24	0.041	1.98	0.40
25	0.042	2.36	0.24
26	0.040	1.31	0.60
28	0.091	1.28	0.47
29	0.089	1.30	0.41
30	0.584	1.00	0.97
31	0.065	1.48	0.61
32	0.078	1.32	0.51
33	0.624	1.16	0.94
34	0.084	1.20	0.81
35	0.184	1.14	0.80
39	0.940	1.05	1.14

<sup>a</sup> Ratio ( $< 1.7$ ) indicates protein contamination.

<sup>b</sup> Ratio ( $< 2.0$ ) indicates humic acid contamination.

Table 4.3: Comparison of DNA yield and purity of a sample with and without dilution of the DNA extracts

Sample and description	DNA yield ( $\mu\text{g}/\mu\text{l}$ )	$A_{260}:A_{280}$ <sup>a</sup>	$A_{260}:A_{230}$ <sup>b</sup>
17 (without DNA dilution)	0.052	1.10	0.7
17 (10-fold DNA dilution)	0.013	0.83	2.5

<sup>a</sup> Ratio ( $< 1.7$ ) indicates protein contamination.

<sup>b</sup> Ratio ( $< 2.0$ ) indicates humic acid contamination.

### 4.3 Amplification of 16S rRNA gene fragments by nested PCR

#### 4.3.1 Primary Polymerase Chain Reaction (PCR)

Bacterial 16S rRNA gene fragments were successfully amplified from the extracted genomic DNA of the samples. The size of the amplicons, which was determined by agarose gel electrophoresis (Figures 4.1a, b and c), was approximately 1500 bp. Samples 8, 9, and 32 showed very faint band intensity while sample 3 showed the brightest band intensity.

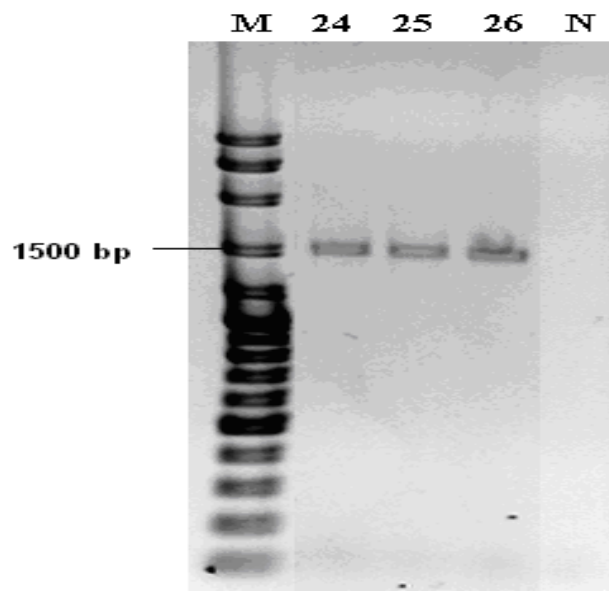


Figure 4.1a: EtBr stained agarose gel 1.0 % (w/v) of primary PCR amplicons of soil and sediment samples 24, 25 and 26. M refers to DNA ladder purchased from Vivantis. N refers to negative control without DNA template.

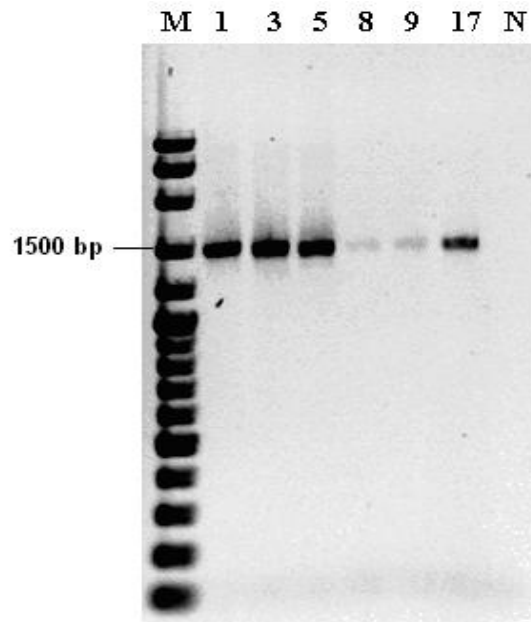


Figure 4.1b: EtBr stained agarose gel 1.0 % (w/v) of primary PCR amplicons of soil and sediment samples 1, 3, 5, 8, 9 and 17. M refers to DNA ladder purchased from Vivantis. N refers to negative control without DNA template.

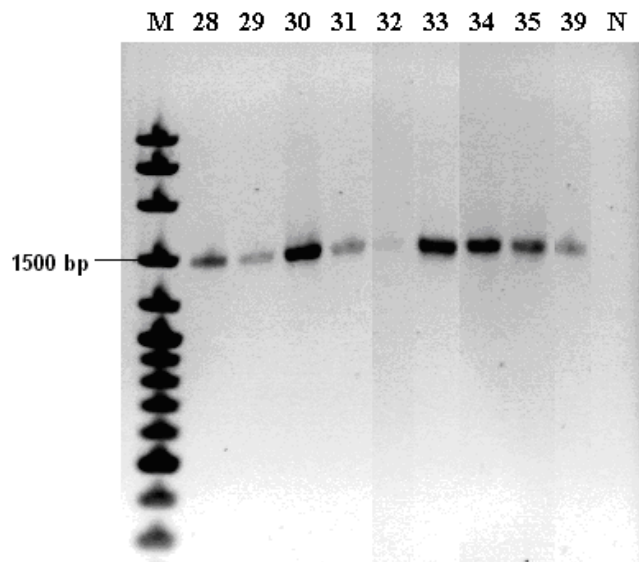


Figure 4.1c: EtBr stained agarose gel 1.0 % (w/v) of primary PCR amplicons of soil and sediment samples 28, 29, 30, 31, 32, 33, 34, 35 and 39. M refers to DNA ladder purchased from Vivantis. N refers to negative control without DNA template.

### **4.3.2 Secondary Polymerase Chain Reaction (PCR)**

Partial bacterial 16S rRNA gene fragments with a GC-rich clamp were successfully amplified from the primary PCR products. The size of the amplicons, which was determined by agarose gel electrophoresis (Figures 4.2a, b and c), was approximately 600 bp. However, fragments larger than 600 bp were also observed, due to the nonspecific binding of primary products during secondary PCR and DNA smear.

For the DGGE, comparison was made between the whole secondary PCR product and the purified excised band at 600 bp only, using two samples (samples 1 and 35). This is to determine if there was any difference in the DGGE patterns when the whole PCR product was used and only the 600 bp band was used.

Unfortunately, fewer bands were observed in DGGE profile when the purified excised band of secondary PCR product was loaded in DGGE, while more bands were observed in DGGE profile when the whole secondary PCR product was loaded in DGGE (Figures 4.3a and b). The purification of 600 bp excised band only for the secondary amplicons might indicate bias to the bacterial DNA in the sample. Some bacterial DNA might have been removed during purification and hence resulting in fewer bands in DGGE profile. Therefore, to analyse and compare the bacterial diversity of samples with minimum bias, the whole secondary PCR product without purification of excised band at 600 bp was loaded in DGGE in this study.

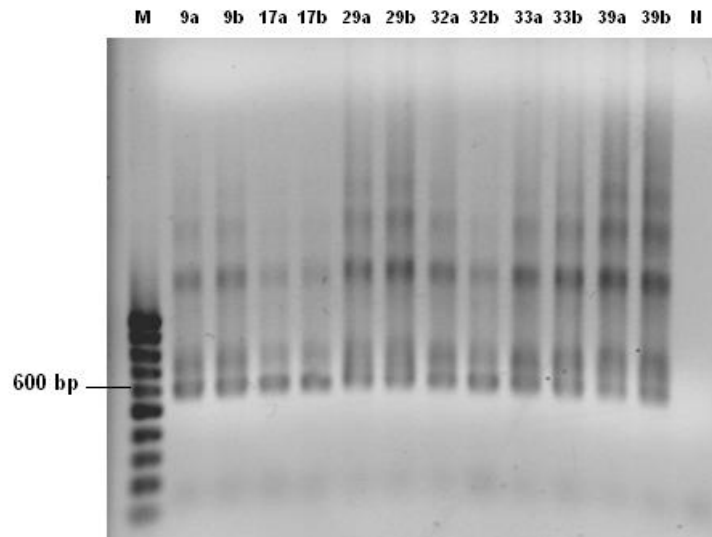


Figure 4.2a: EtBr stained agarose gel 1.0 % (w/v) of secondary PCR amplicons of soil and sediment samples 9, 17, 29, 32, 33 and 39 with replicates (a, b). M refers to DNA ladder purchased from Norgen Biotech Corporation. N refers to negative control with negative control from primary PCR as template.

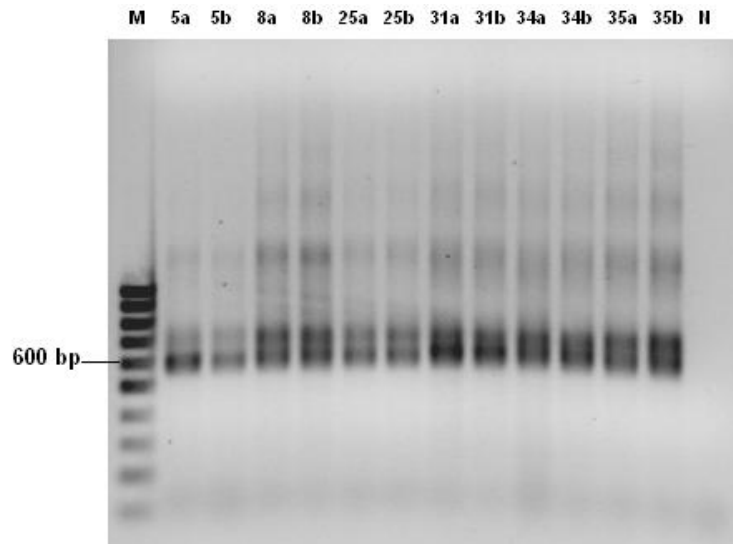


Figure 4.2b: EtBr stained agarose gel 1.0 % (w/v) of secondary PCR amplicons of soil and sediment samples 5, 8, 25, 31, 34 and 35 with replicates (a, b). M refers to DNA ladder purchased from Norgen Biotech Corporation. N refers to negative control with negative control from primary PCR as template.



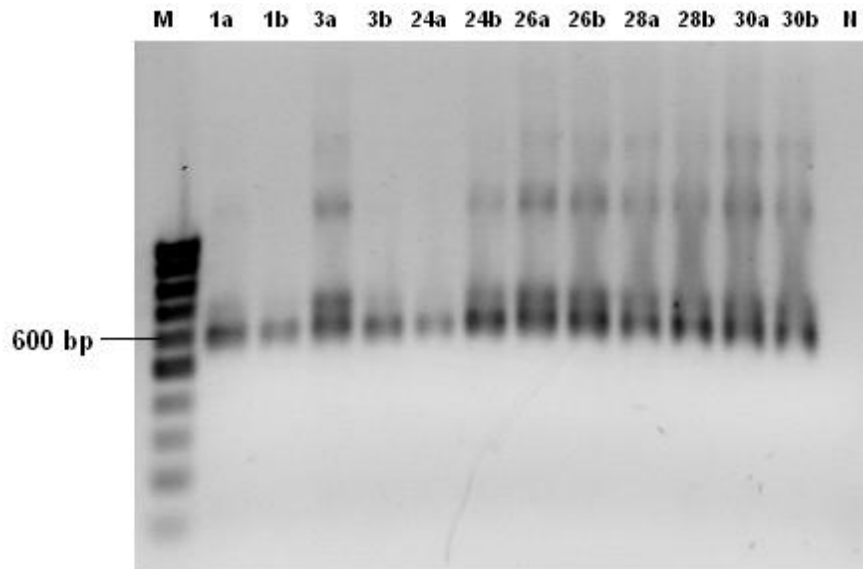


Figure 4.2c: EtBr stained agarose gel 1.0 % (w/v) of secondary PCR amplicons of soil and sediment samples 1, 3, 24, 26, 28 and 30 with replicates (a, b). M refers to DNA ladder purchased from Norgen Biotech Corporation. N refers to negative control with negative control from primary PCR as template.

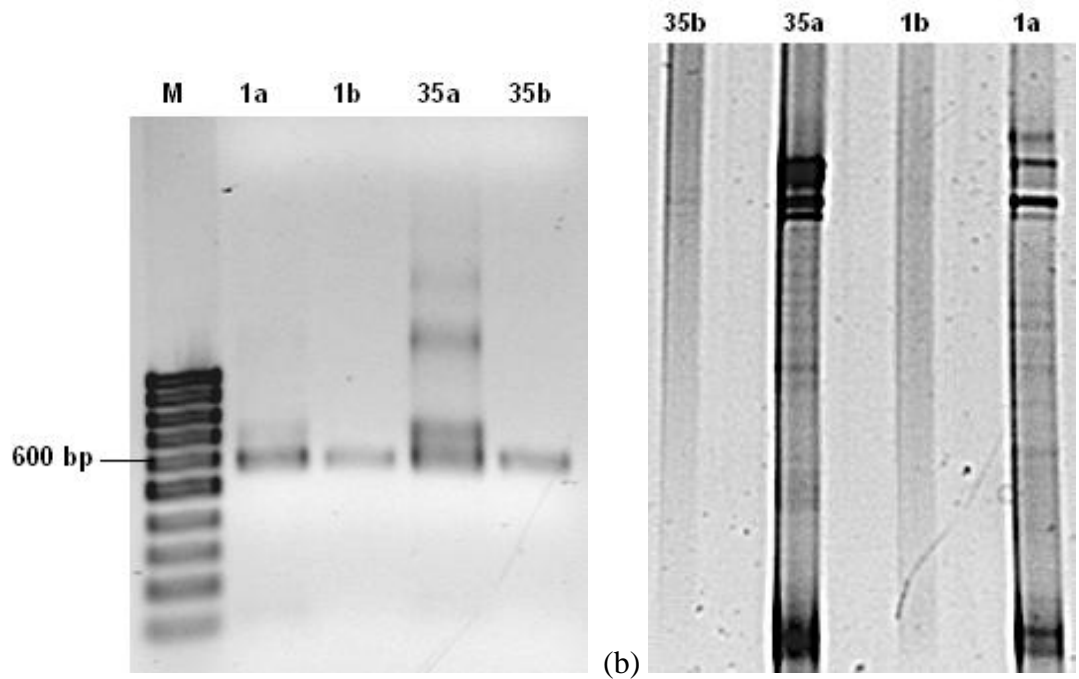


Figure 4.3: (a) Comparison of EtBr stained agarose gel 1.0 % (w/v) of whole secondary PCR amplicons (1a, 35a) and the purified excised band of secondary PCR amplicons at 600 bp only (1b, 35b) of soils and sediments. M refers to DNA ladder purchased from Norgen Biotech Corporation. N refers to negative control with negative control from primary PCR as template. (b) Comparison of DGGE banding pattern between the whole secondary PCR product (1a and 35a) and the purified excised band at 600 bp only (1b and 35b).

#### 4.4 Denaturing Gradient Gel Electrophoresis (DGGE) analysis

##### 4.4.1 Comparison of DGGE banding pattern on sample with and without dilution of DNA template in PCR

DGGE was carried out on PCR amplicons of an undiluted sample and 10-fold diluted sample. Figure 4.4 shows a comparison of DGGE banding pattern of the sample with and without dilution of DNA template. A clearer banding pattern was observed in DGGE profile of sample DNA that had been diluted 10-fold in PCR.

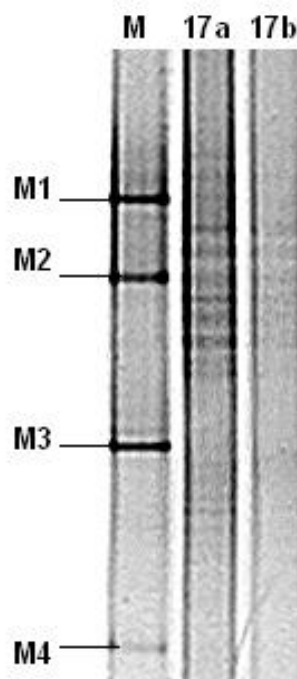


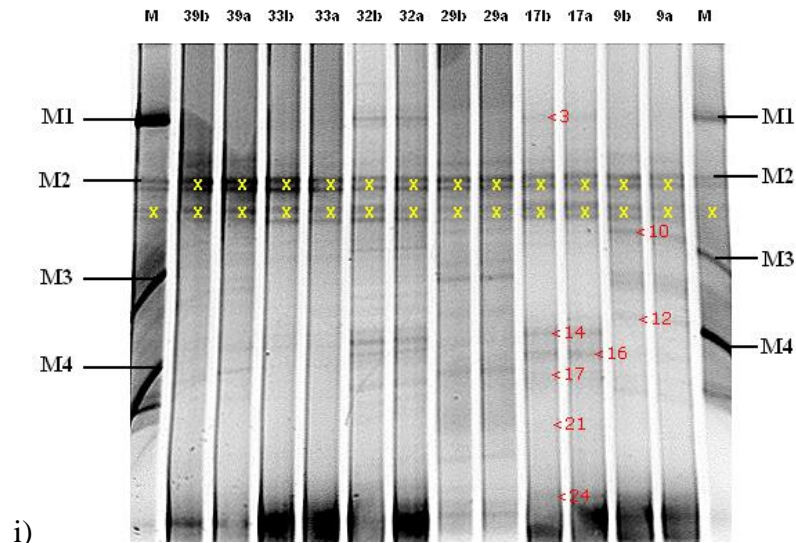
Figure 4.4: Comparison of DGGE banding pattern with and without dilution of DNA template. M1 to M4 refer to bands with distinct melting position from the previous DGGE run as markers on the gel. 17a refers to PCR amplicon from 10-fold diluted DNA template. 17b refers to PCR amplicon from non-diluted DNA template.

#### **4.4.2 Comparison of DGGE banding pattern between the samples**

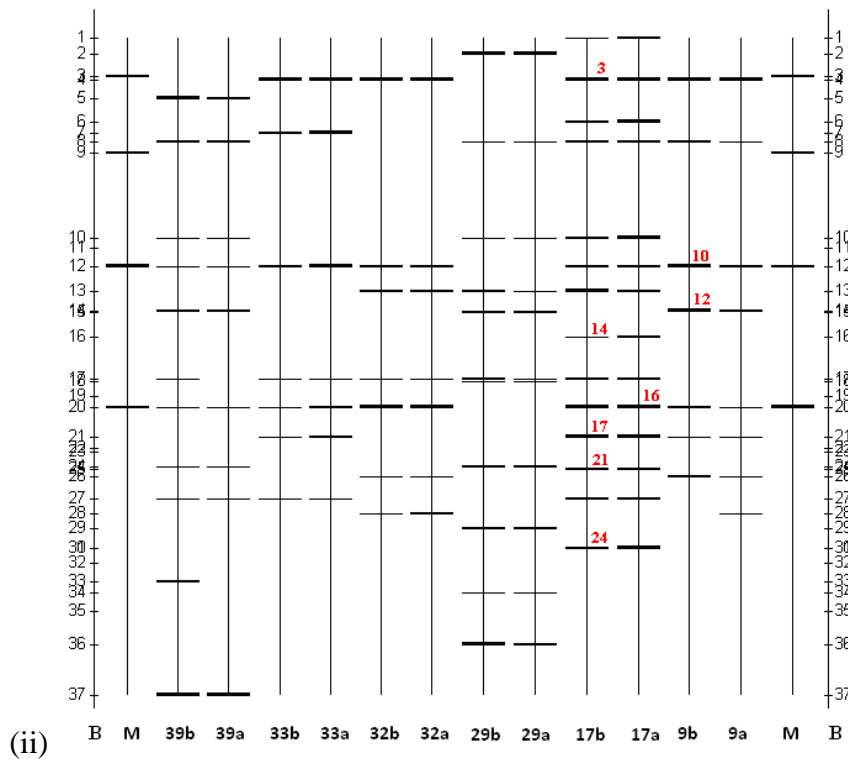
DGGE was carried on the secondary PCR amplicons to analyse the bacterial diversity from different soil and sediment samples (Figures 4.5a, b and c). The DGGE banding pattern was different among samples. For instance, sample 17 showed the highest number of bands but the banding pattern was not distributed, while sample 39 showed lower number of bands but the banding pattern was widely distributed (Figure 4.5a).

The numbers (in red) against a band refer to well-defined bands that were excised for sequencing; in order to identify the bacterial species that represented the band. Theoretically, bacterial species that represented a well-defined band was present in other samples that had the same position with the well-defined band. For instance, band 1 (banding position 2) were also present in samples 1, 5 and 29 although the band was excised from sample 25.

Artificial bands that were at the location of M2 and below M2, were observed in all samples.

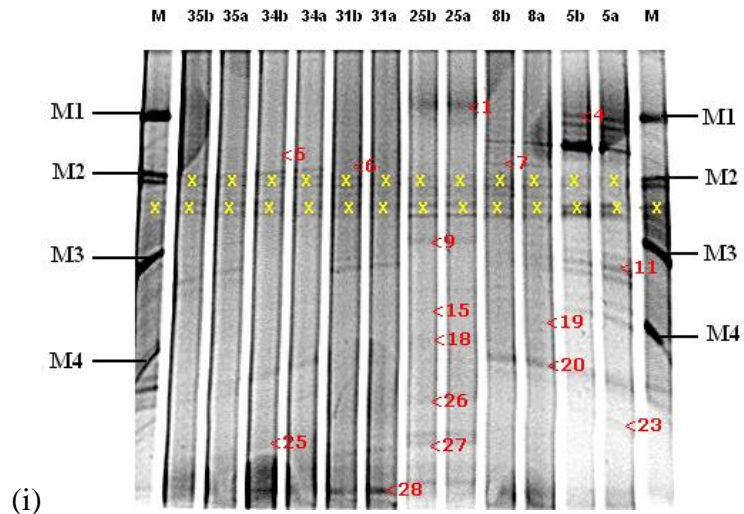


i)

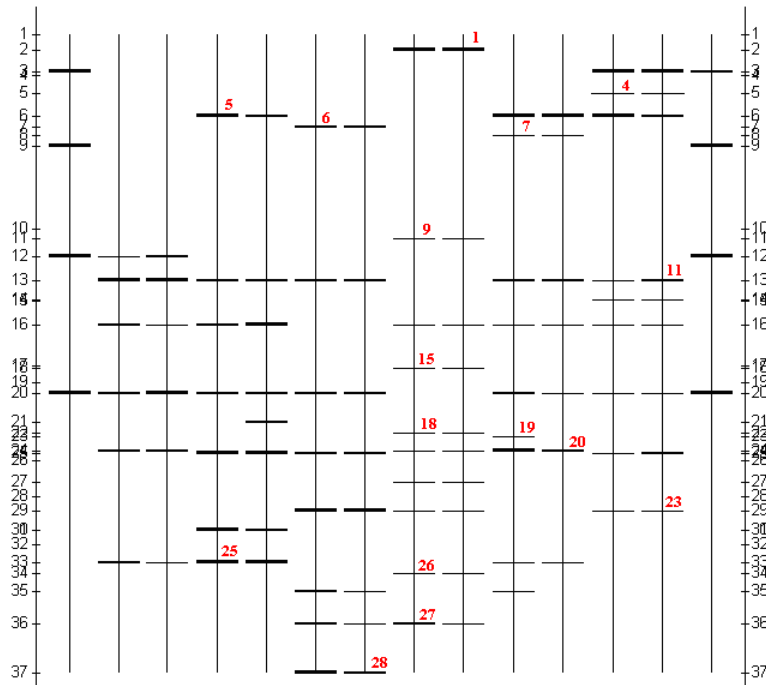


(ii)

Figure 4.5a: DGGE profile (i) and schematic picture (ii) of 16S rDNA fragments amplified from samples (39=melt lake, 33=higher level periglacier, 32=periglacier, 29=middle layer of marine sediment from 20 m depth site, 17=tundra and 9=dry tundra) with replicates (a, b). M1 to M4 refer to bands with distinct melting position from the previous DGGE run as markers on the gel. Numbers (in red) against a band refer to well-defined bands excised for sequencing. A yellow “X” against a band refers to an artificial band.



(i)



(ii)

Figure 4.5b: DGGE profile (i) and schematic picture (ii) of 16S rDNA fragments amplified from samples (35=freshwater inland lake, 34=old mine mound, 31=lower level periglacier, 25=middle layer of marine sediment from 10 m depth site, 8=storvanet inland lake and 5=runnel) with replicates (a, b). M1 to M4 refer to bands with distinct melting position from the previous DGGE run as markers on the gel. Numbers (in red) against a band refer to well-defined bands excised for sequencing. A yellow “X” against a band refers to an artificial band.

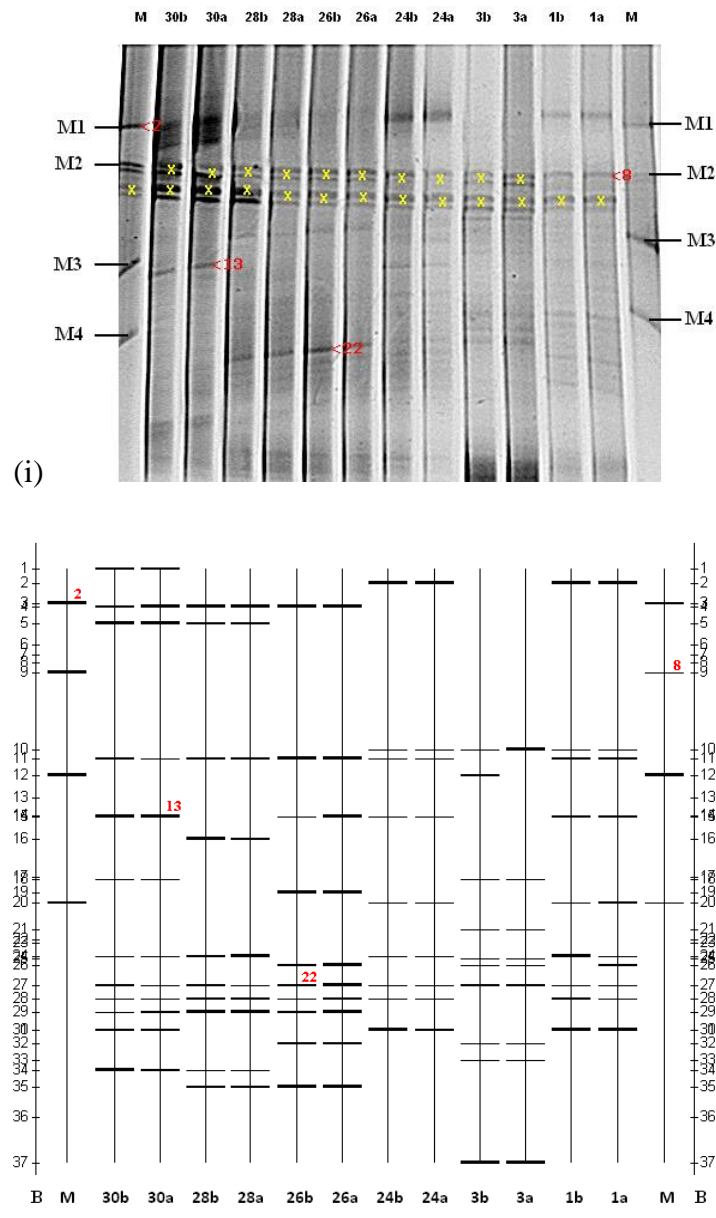


Figure 4.5c: DGGE profile (i) and schematic picture (ii) of 16S rDNA fragments amplified from samples (30=lower layer of marine sediment from 20 m depth site, 28=top layer of marine sediment from 20 m depth site, 26=lower layer of marine sediment from 10 m depth site, 24=top layer of marine sediment from 10 m depth site, 3=rail track and 1=harbour) with replicates (a, b). M1 to M4 refer to bands with distinct melting position from the previous DGGE run as markers on the gel. Numbers (in red) against a band refer to well-defined bands excised for sequencing. A yellow “X” against a band refers to an artificial band.

## **4.5 Statistical analysis of DGGE profiles**

### **4.5.1 Comparison of bacterial diversity between the samples**

The DGGE profiles were transformed into a presence/absence binary matrix. Table 4.4 shows the occurrence frequency of bands within each sample resulted from the presence/absence binary matrix. The number of accumulated bands (species richness) in each sample indicating number of dominant bacteria in the sample, and can be used for comparison purpose (Muller *et al.*, 2001; Van Der Gucht *et al.*, 2001). The number of “0”s refer to the absence of bands, whereas the number of “2”s indicate that two specific bands were detected in all two replicates. A total of 37 DGGE banding positions were detected from all sampling sites, and the identities of 28 bands were determined, as indicated in the DGGE profiles. Some samples had the same number of detected bands. For instance, a total of 20 bands were detected in marine (samples 25, 26 and 28) and melt lake (sample 39) samples. The highest occurrence frequency of bands (TB = 28) was shown in terrestrial sample from the tundra site (sample 17) whereas the lowest occurrence frequency of bands (TB = 12) was shown in inland lake bank sample from the freshwater site (sample 35).



Table 4.4: Occurrence frequency of bands within each sample obtained from the presence/absence binary matrix

	<b>30</b>	<b>28</b>	<b>26</b>	<b>24</b>	<b>3</b>	<b>1</b>	<b>39</b>	<b>33</b>	<b>32</b>	<b>29</b>	<b>17</b>	<b>9</b>	<b>35</b>	<b>34</b>	<b>31</b>	<b>25</b>	<b>8</b>	<b>5</b>
<b>1</b>	2	0	0	0	0	0	0	0	0	0	2	0	0	0	0	0	0	0
<b>2</b>	0	0	0	2	0	2	0	0	0	2	0	0	0	0	0	2	0	0
<b>3</b>	0	0	0	0	0	0	0	0	0	0	0	0	0	0	0	0	0	2
<b>4</b>	2	2	2	0	0	0	0	2	2	0	2	2	0	0	0	0	0	0
<b>5</b>	2	2	0	0	0	0	2	0	0	0	0	0	0	0	0	0	0	2
<b>6</b>	0	0	0	0	0	0	0	0	0	0	2	0	0	2	0	0	2	2
<b>7</b>	0	0	0	0	0	0	0	2	0	0	0	0	0	0	2	0	0	0
<b>8</b>	0	0	0	0	0	0	2	0	0	2	2	2	0	0	0	0	2	0
<b>9</b>	0	0	0	0	0	0	0	0	0	0	0	0	0	0	0	0	0	0
<b>10</b>	0	0	0	2	2	2	2	0	0	2	2	0	0	0	0	0	0	0
<b>11</b>	2	2	2	2	0	2	0	0	0	0	0	0	0	0	0	2	0	0
<b>12</b>	0	0	0	0	1	0	2	2	2	0	2	2	2	0	0	0	0	0
<b>13</b>	0	0	0	0	0	0	0	0	2	2	2	0	2	2	2	0	2	2
<b>14</b>	0	0	0	0	0	0	2	0	0	0	0	2	0	0	0	0	0	2
<b>15</b>	2	0	2	2	0	2	0	0	0	2	0	0	0	0	0	0	0	0
<b>16</b>	0	2	0	0	0	0	0	0	0	0	2	0	2	2	0	2	2	2
<b>17</b>	0	0	0	0	0	0	1	2	2	2	2	0	0	0	0	0	0	0
<b>18</b>	2	0	0	0	2	0	0	0	0	2	0	0	0	0	0	2	0	0
<b>19</b>	0	0	2	0	0	0	0	0	0	0	0	0	0	0	0	0	0	0
<b>20</b>	0	0	0	2	0	2	2	2	2	0	2	2	2	2	2	0	2	2
<b>21</b>	0	0	0	0	2	0	0	2	0	0	2	2	0	1	0	0	0	0
<b>22</b>	0	0	0	0	0	0	0	0	0	0	0	0	0	0	0	2	0	0
<b>23</b>	0	0	0	0	0	0	0	0	0	0	0	0	0	0	0	0	1	0
<b>24</b>	2	2	0	2	0	2	2	0	0	2	0	0	2	0	0	2	2	0
<b>25</b>	0	0	0	0	2	0	0	0	0	0	2	0	0	2	2	0	0	2
<b>26</b>	0	0	2	0	2	1	0	0	2	0	0	2	0	0	0	0	0	0
<b>27</b>	2	2	2	2	2	2	2	2	0	0	2	0	0	0	0	2	0	0
<b>28</b>	2	2	2	2	0	2	0	0	2	0	0	1	0	0	0	0	0	0
<b>29</b>	2	2	2	0	0	0	0	0	0	2	0	0	0	0	2	2	0	2
<b>30</b>	2	0	0	2	0	2	0	0	0	0	0	0	0	0	0	0	0	0
<b>31</b>	0	0	0	0	0	0	0	0	0	0	2	0	0	2	0	0	0	0
<b>32</b>	0	0	2	0	2	0	0	0	0	0	0	0	0	0	0	0	0	0
<b>33</b>	0	0	0	0	2	0	1	0	0	0	0	0	2	2	0	0	2	0
<b>34</b>	2	2	0	0	0	0	0	0	0	2	0	0	0	0	0	2	0	0
<b>35</b>	0	2	2	0	0	0	0	0	0	0	0	0	0	0	2	0	1	0
<b>36</b>	0	0	0	0	0	0	0	0	0	2	0	0	0	0	2	2	0	0
<b>37</b>	0	0	0	0	2	0	2	0	0	0	0	0	0	0	2	0	0	0
<b>TB<sup>a</sup></b>	<b>24</b>	<b>20</b>	<b>20</b>	<b>18</b>	<b>19</b>	<b>19</b>	<b>20</b>	<b>14</b>	<b>14</b>	<b>22</b>	<b>28</b>	<b>15</b>	<b>12</b>	<b>15</b>	<b>16</b>	<b>20</b>	<b>16</b>	<b>18</b>

Column numbers refer to the sample. Row numbers refer to the banding position in DGGE profiles.

<sup>a</sup>Total accumulated bands from each sample with 2 replicates

The data obtained from presence/absence binary matrix (Table 4.4) was then used to generate Non-metric Multidimensional Scaling (nMDS) plots, Hierarchical cluster analysis and Shannon diversity index ( $H'$ ).

The nMDS plots of DGGE profile (Figure 4.6) and the Hierarchical cluster analysis (Figure 4.7) was determined to compare the similarity in the bacterial communities between samples. The samples studied were clustered into two main groups: non-marine (samples 3, 5, 8, 9, 17, 31, 32, 33, 34, 35 and 39) and marine samples (samples 1, 24, 25, 26, 28, 29 and 30) with approximately 20 % similarity. Bacterial community structure of the non-marine samples such as terrestrial, periglacier, inland lake bank and melt lake bank samples were found to be around 30% similar to each other. Samples from the lower level site of periglacier (sample 31) and rail track site (sample 3) were distinct from other studied sites. The highest similarity (> 90 %) was detected between beach soil (sample 1) and marine sediment (sample 24). More than 60 % similarity was shown in between dry tundra terrestrial sample (sample 9) and periglacier samples (sample 32); in between inland lake bank samples (samples 8 and 35); and in between terrestrial samples (samples 5 and 34). The diversity of the melt lake sediment (sample 39) was approximately 40% similar to the periglacier soils (sample 32 and 33).

$H'$  inferred from DGGE binary matrices data was used to compare the dominant bacterial diversity in the studied samples (Table 4.5). In brief, higher  $H'$  indicated greater bacterial diversity while lower  $H'$  indicated lower diversity. The highest Shannon diversity index ( $H' = 2.639$ ) was observed in the tundra terrestrial sample (sample 17), while the lowest Shannon diversity index ( $H' = 1.792$ ) was observed in the freshwater inland lake bank sample (sample 35). A slightly increases of Shannon diversity index in marine samples ( $H' = 2.197$  to  $H' = 2.485$ ), was shown from an upper depth site (sample 24), to the lower depth site (sample 30).

It is perhaps noteworthy that these data need to be handled with care as  $H'$  value inferred directly from the DGGE presence/absence binary data might not reflect the true diversity in the soils and sediments (Chong *et al.*, 2009b). (Further discussion in Section 5.4). Nevertheless,  $H'$  is used here to allow a coarse comparison of “diversity richness” between studied samples.

## Bacterial Diversity of Eighteen Sites in Ny-Ålesund

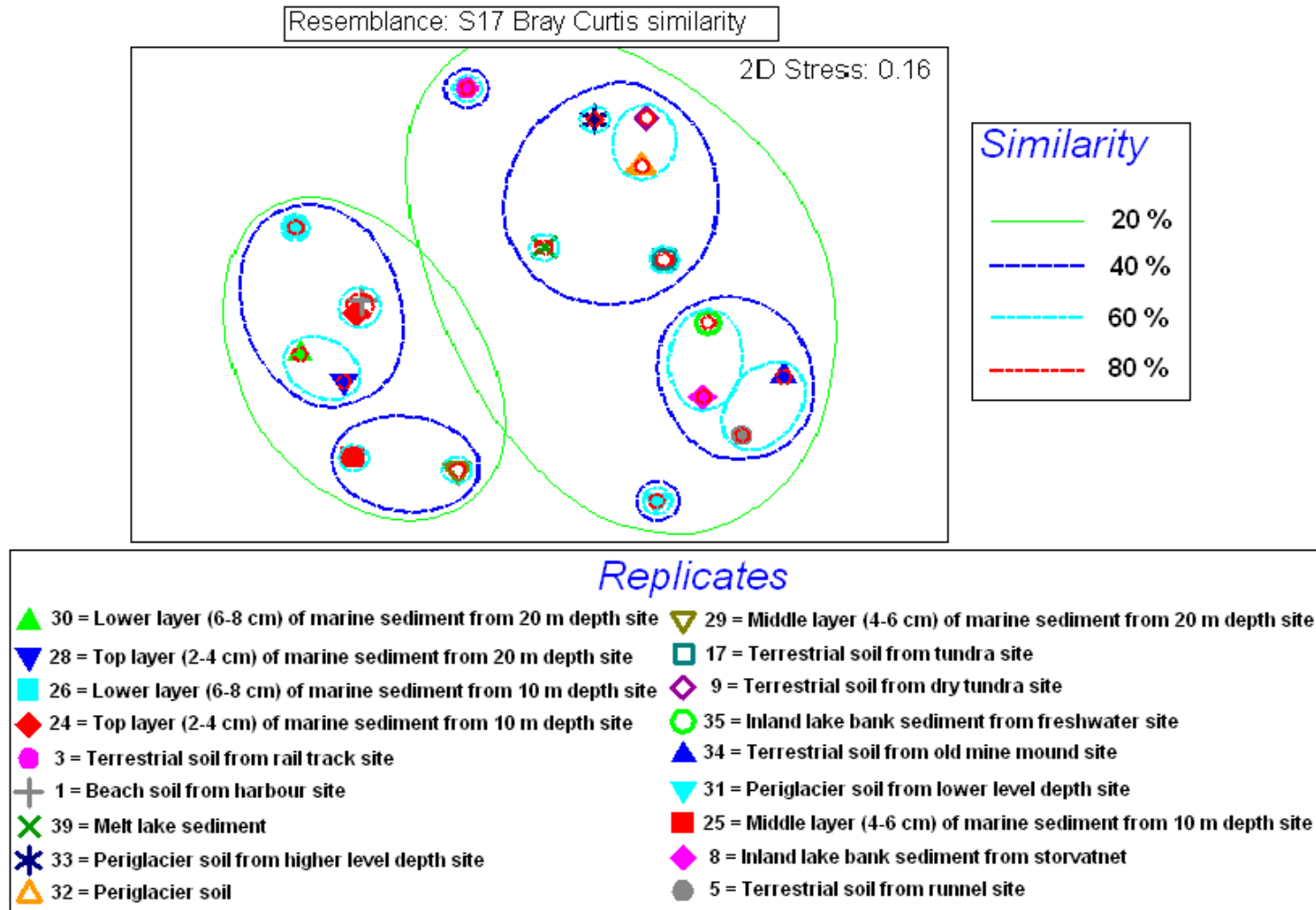


Figure 4.6: Non-metric multidimensional scaling (nMDS) plots of DGGE profiles based on a presence/absence binary matrix.



Table 4.5: Shannon diversity index ( $H'$ ) calculation inferred from the presence/absence binary matrix

Sample	Total species ( $S$ ) <sup>a</sup>	Total individuals ( $N$ ) <sup>b</sup>	Species richness ( $d$ ) <sup>c</sup>	Pielou's evenness ( $J'$ ) <sup>d</sup>	Shanon diversity index ( $H'$ ) <sup>e</sup>
35	6	12	2.012	1	1.792
31	7	14	2.274	1	1.946
32	7	14	2.274	1	1.946
33	7	14	2.274	1	1.946
9	8	15	2.585	0.9912	2.061
34	8	15	2.585	0.9912	2.061
8	9	16	2.885	0.9858	2.166
3	9	17	2.824	0.9925	2.181
5	9	18	2.768	1	2.197
24	9	18	2.768	1	2.197
39	10	18	3.114	0.9877	2.274
1	10	19	3.057	0.9936	2.288
25	10	20	3.004	1	2.303
26	10	20	3.004	1	2.303
28	10	20	3.004	1	2.303
29	11	22	3.235	1	2.398
30	12	24	3.461	1	2.485
17	14	28	3.901	1	2.639

<sup>a</sup>  $S$  = the number of banding position (species) in each sample

<sup>b</sup>  $N$  = total number of accumulated bands in each sample

<sup>c</sup>  $d = (S - 1) / \ln N$

<sup>d</sup>  $J' = H' / \ln S$

<sup>e</sup>  $H' = - \sum Pi \ln (Pi)$  where  $Pi$  is the proportion of the  $i$ th species in each sample

#### 4.5.2 Correlation of bacterial diversity and environmental variables

The Biota and/or Environment matching (BEST) procedure, based on Spearman rank correlations (Table 4.6), gave results on the correlation between the environmental variables (Table 4.1) and the bacterial diversity of the samples (Table 4.4). Spearman rank order correlation showed significant correlations ( $P = 0.001$ ) between samples electrical conductivity ( $r = 0.470$ ) and pH ( $r = 0.294$ ) with the bacterial diversity. Environmental multiple variables (combination of pH and electrical conductivity) showed higher correlation ( $r = 0.469$ ) to the bacterial diversity than that of only electrical conductivity.

Table 4.6: BEST result on correlations of environmental variables with the bacterial diversity (Global  $r = 0.470^a$ ;  $P = 0.001^b$ )

	Variables	Correlation coefficients
Single variables	pH	0.470
	Electrical conductivity	0.294
Multiple variables	pH and electrical conductivity	0.469

The BEST result was based on <sup>a</sup> Spearman rank correlation with a <sup>b</sup> significant level

#### 4.6 Recovery and purification of well-defined DGGE bands

Well-defined DGGE bands were successfully recovered by PCR without GC-clamp and purified using Gel DNA Recovery Kit. The size of the purified products, which was determined by agarose gel electrophoresis, was approximately 600 bp (Figures 4.8a, b and c). Some purified products had a brighter band intensity (Bands 4, 13 and 28), which might have been due to their brighter DGGE band intensity.

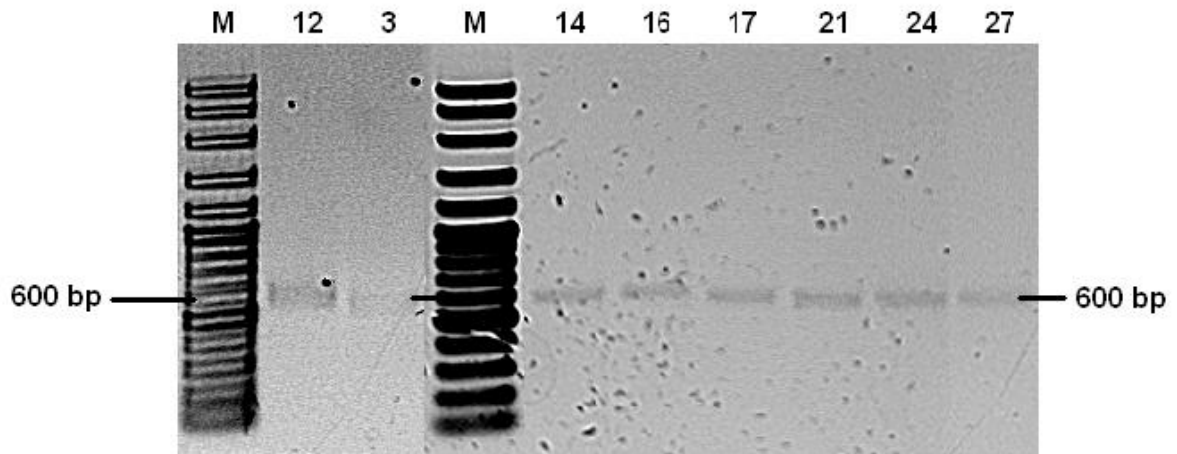


Figure 4.8a: EtBr stained agarose gel 1.0 % (w/v) of purified DGGE well-defined bands (bands 3, 12, 14, 16, 17, 21, 24 and 27). M refers to DNA ladder purchased from Vivantis.

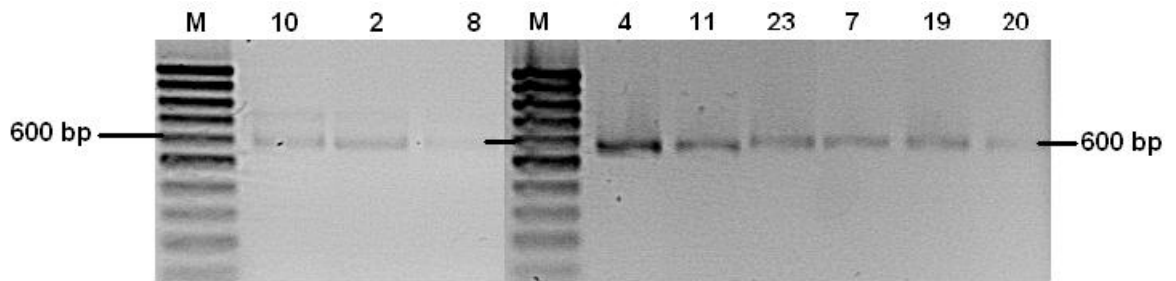


Figure 4.8b: EtBr stained agarose gel 1.0 % (w/v) of purified DGGE well-defined bands (bands 2, 4, 7, 8, 10, 11, 19, 20 and 23). M refers to DNA ladder purchased from Norgen Biotech Corporation.

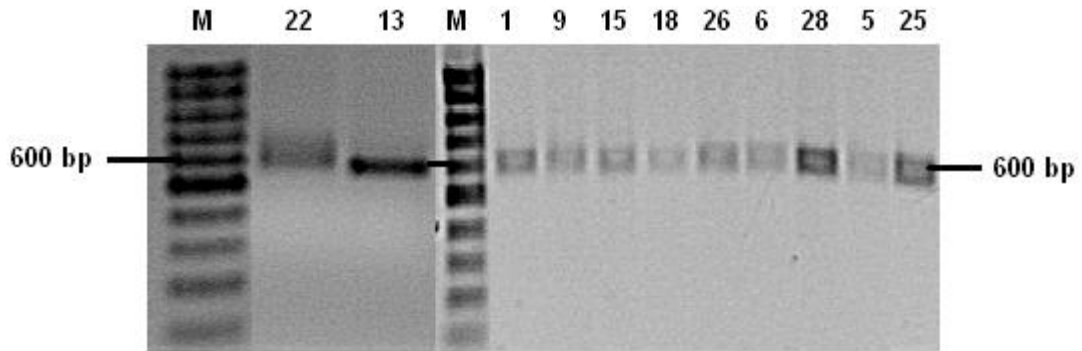


Figure 4.8c: EtBr stained agarose gel 1.0 % (w/v) of purified DGGE well-defined bands (bands 1, 5, 6, 9, 13, 15, 18, 22, 25, 26 and 28). M refers to DNA ladder purchased from Norgen Biotech Corporation.



#### 4.7 16S rRNA gene fragment analysis and phylogenetic analysis

The well-defined DGGE bands were identified using BLAST search in GenBank (Table 4.7). The well-defined DGGE bands showed 71 % to 100 % homology to a wide range of uncultured bacteria available in GenBank database. Out of 28 DGGE bands that were sequenced, four sequences each were related to *Bacteroidetes* and  *$\beta$ -proteobacteria*, two each were related to *Cyanobacteria*, *Firmicutes* and *Fusobacteria*, and one each were related to *Acidobacteria*,  *$\epsilon$ -proteobacteria*,  *$\delta$ -proteobacteria*, *Fibrobacteres* and *Nitrospira*. In additions, nine sequences were unable to classify into any known phylum.

Sequences related to *Bacteroidetes* (banding positions 2, 4, 11 and 12), unclassified bacteria (banding positions 3, 6, 8, 13, 14, 22, 23, 27 and 29) and *Fibrobacteres* (banding position 20) were found in all samples studied. *Acidobacteria* (banding position 30) were found in terrestrial, beach, and marine samples but not identified in periglacier and melt lake samples. *B-proteobacteria* (banding positions 7, 21, 33 and 37) were found in non-marine group samples but not identified in marine group samples, while  *$\epsilon$ -proteobacteria* (banding position 15) were found in marine group samples but not identified in non-marine group samples.

*Cyanobacteria* (banding positions 5 and 16) were found only in terrestrial, inland lake bank, melt lake, and marine samples; *Firmicutes* (banding positions 9 and 24) in inland lake bank, beach, melt lake, and marine samples; *Fusobacteria* (banding positions 17 and 34) in terrestrial, periglacier, melt lake, and marine samples;  *$\delta$ -proteobacteria* (banding position 36) in periglacier and marine samples; and *Nitrospira* (banding position 25) in terrestrial and periglacier samples.

Figure 4.9 shows the phylogenetic analysis of the well-defined DGGE bands, using Neighbor-Joining algorithm of 1000 replicates with a scale length of 0.05. Only bootstrap values of more than 50 are shown. There were four distinct clades displayed in the

phylogenetic tree, which consisted of (i) members of *Bacteroidetes* and *Cyanobacteria* (ii) members of *Firmicutes*, *Nitrospira*, *Fibrobacteres*, *Acidobacteria*,  $\epsilon$ -*proteobacteria* and  $\delta$ -*proteobacteria*; (iii) members of  $\beta$ -*proteobacteria*; and (iv) members of *Fusobacteria*. *Bacteroidetes* and *Cyanobacteria* were cluster together (50 % confidence).  $\beta$ -*proteobacteria* were not closely related with  $\delta$ -*proteobacteria* and  $\epsilon$ -*proteobacteria*. There was a distinct clade of unidentified representative (banding positions 8, 13, 14, 22, 23, 27 and 29) that was not closely related to any known bacteria sequences in GenBank BLAST.

Table 4.7: Identification of sequences of well-defined DGGE bands using BLAST search in GenBank

DGGE band number	DGGE banding position	Available in sample (M <sup>a</sup> , T <sup>b</sup> , I <sup>c</sup> , P <sup>d</sup> , B <sup>e</sup> , ML <sup>f</sup> )	Nearest match (Accession number)	Phylum/Class <sup>g</sup>	Source	% H <sup>h</sup>
1	2	M, B	Uncultured <i>Cytophaga</i> sp.; clone JTB132 (AB015260)	<i>Bacteroidetes</i>	Deepest cold-seep, Japan	97
2	3	T	Uncultured bacterium; clone MBA3 (EU044921)	unclassified	Canadian Arctic microbial mat	90
3	4	M, T, P	Uncultured <i>Sphingobacteriaceae</i> bacterium; RUGL1-492 (GQ420939)	<i>Bacteroidetes</i>	Himalayas glacier	97
4	5	M, T, ML	Uncultured Cyanobacterium; BAC_2_B08 (FJ967911)	<i>Cyanobacteria</i>	Cold sulphur rich spring water, Michigan	99
5	6	T, I	Uncultured <i>Bacteroidetes</i> bacterium; P249 (DQ263545)	unclassified	Pine soil, California	94
6	7	P	Uncultured <i>Comamonadaceae</i> bacterium; GC12m-4-86 (EU641093)	<i>β-proteobacteria</i>	Environmental sample	89
7	8	M, T, I, ML	Uncultured Cyanobacterium; CYAK01 (FJ774024)	unclassified	Lake Marathon water	94
8	9	-	Uncultured <i>Clostridia</i> bacterium (EF034966)	<i>Firmicutes</i>	Spitsbergen permafrost soil	98
9	11	M, B	Uncultured <i>Flavobacteria</i> bacterium (AM279186)	<i>Bacteroidetes</i>	Marine water, Germany	91
10	12	T, I, P, ML	Uncultured <i>Bacteroidetes</i> bacterium; SI-1F_G11 (EF221319)	<i>Bacteroidetes</i>	Unvegetated soil, Signy Island	92
11	13	M, T, I, P	Uncultured Cyanobacterium; CYAK01 (FJ774024)	unclassified	Lake Marathon	93
12	14	T, ML	Uncultured Beta Proteobacterium; G09_WMSP1 (DQ450777)	unclassified	Alpine tundra soil	81

Table 4.7, Continued

13	15	M, B	Uncultured Epsilon Proteobacterium gene (AB013262)	<i>ε-proteobacteria</i>	Nankai Trough sediments, Japan	99
14	16	M, T, I	<i>Microcoleus vaginatus</i> ; OTA3-2 clone 148-4B (AF355373)	<i>Cyanobacteria</i>	Environmental sample	97
15	17	M, T, P, ML	Uncultured <i>Fusobacteria</i> bacterium (AJ575990)	<i>Fusobacteria</i>	Deep sea hydrothermal vent	95
16	20	M, T, I, P, B, ML	Uncultured <i>Fibrobacteres</i> bacterium; GASP-WC2W3_H08 (EF075320)	<i>Fibrobacteres</i>	Environmental sample	93
17	21	T, P	Uncultured <i>Polaromonas</i> sp.; LSS-C2 (FJ946515)	<i>β-proteobacteria</i>	Arctic snow, Norway	100
18	22	M	Uncultured <i>Fusobacteria</i> bacterium (AJ575990)	unclassified	Deep sea hydrothermal vent	98
19	23	I	Uncultured Cyanobacterium; SPU243 (EU728976)	unclassified	High altitude lake, Bolivia	96
20	24	M, I, B, ML	Uncultured <i>Firmicutes</i> bacterium; ANTXXIII_706-4_Bac93 (FN429808)	<i>Firmicutes</i>	Marine sediment, Antarctica	90
21	25	T, P	Uncultured <i>Nitrospiraceae</i> bacterium; sw-xj228 (GQ302558)	<i>Nitrospira</i>	Cold spring sediment	99
22	27	M, T, P, B, ML	Uncultured Alpha Proteobacterium; T31_1 (DQ436537)	unclassified	Mediterranean seawater	71
23	29	M, T, P	Uncultured <i>Comamonadaceae</i> bacterium; BF M20(8) (DQ628936)	unclassified	John Evans glacier water, Canada	88
24	30	M, T, P	Uncultured <i>Acidobacterium</i> sp.; RUGL6-235 (GQ366546)	<i>Acidobacteria</i>	Himalayas glacier	95
25	33	T, I, ML	<i>Burkholderiales</i> bacterium; TP366 (EF636119)	<i>β-proteobacteria</i>	Freshwater pond sediment	93
26	34	M	Uncultured <i>Fusobacteria</i> bacterium (AJ575990)	<i>Fusobacteria</i>	Deep sea hydrothermal vent	96

Table 4.7, Continued

27	36	M, P	Uncultured Delta Proteobacterium; clone ANTXIII_706-4_Bac26 (FN429801)	<i>δ-proteobacteria</i>	Marine sediment, Antarctica	94
28	37	T, P, ML	Uncultured Beta Proteobacterium; MEf05cnp11C3 (FJ828023)	<i>β-proteobacteria</i>	Environmental sample	97

<sup>a</sup> Marine sediments

<sup>b</sup> Terrestrial soils

<sup>c</sup> Inland lake bank sediments

<sup>d</sup> Periglacier soils

<sup>e</sup> Beach soil

<sup>f</sup> Melt lake sediment

<sup>g</sup> Taxonomic classification based on Ribosomal Database Project 10 classifier, the confident threshold was set at 80%

<sup>h</sup> Percent homology with reference sequence in GenBank databse

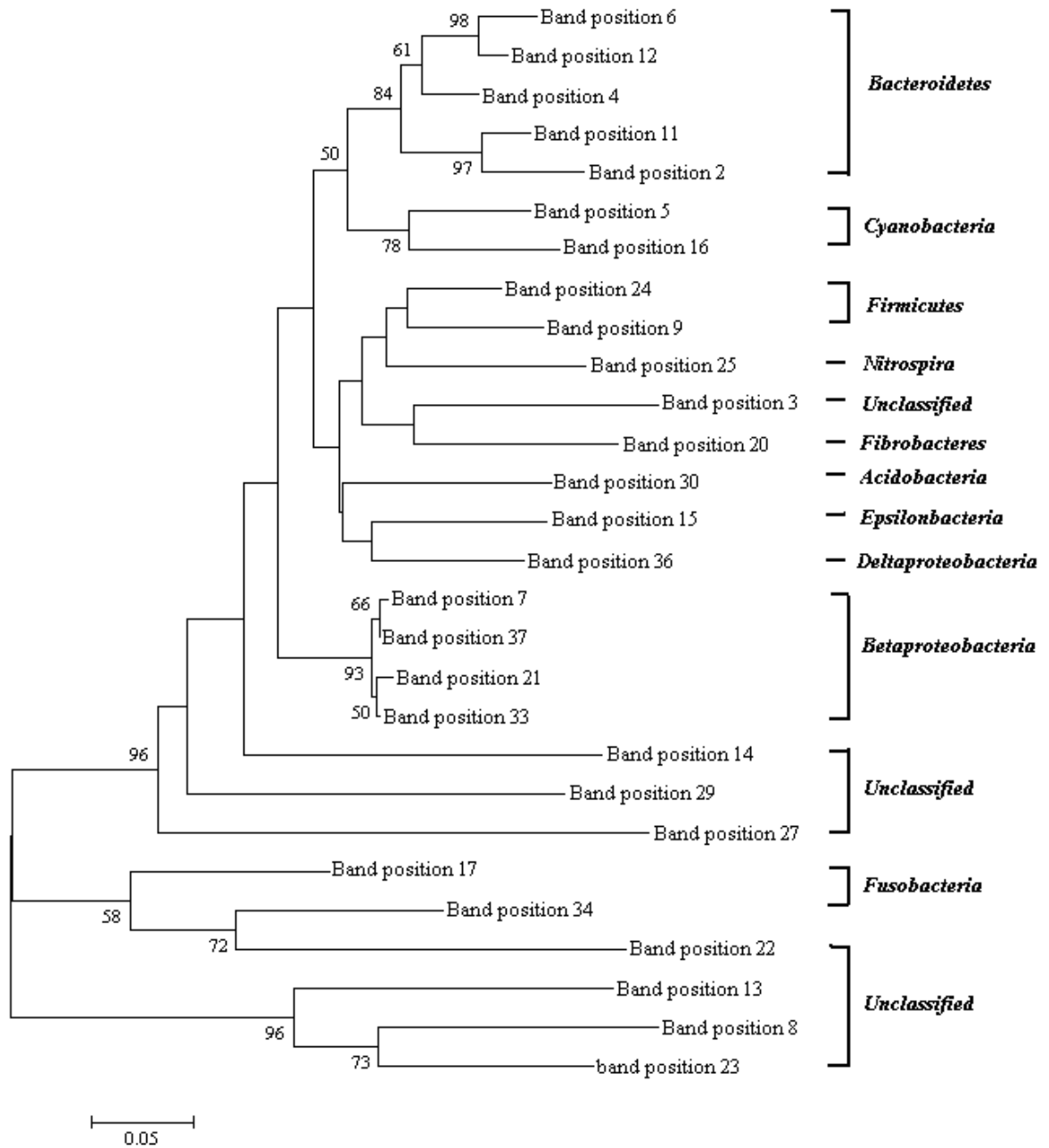


Figure 4.9: Phylogenetic analysis of sequenced DGGE bands (~200 bp) using Neighbor-Joining algorithm and 1000 re-sampling replicates with a scale length 0.05. Only bootstrap values of more than 50 % are shown.